Molecular Biology of the Cell
Vol. 14, 4329–4341, November 2003

Urmylation: A Ubiquitin-like Pathway that Functions during Invasive Growth and Budding in Yeast

April S. Goehring,* David M. Rivers, and George F. Sprague, Jr.†

Institute of Molecular Biology, University of Oregon, Eugene, Oregon 97403-1229

Submitted February 11, 2003; Revised June 5, 2003; Accepted June 26, 2003
Monitoring Editor: Trisha Davis

Ubiquitin is a small modifier protein that is conjugated to substrates to target them for degradation. Recently, a surprising number of ubiquitin-like proteins have been identified that also can be attached to proteins. Herein, we identify two molecular functions for the posttranslational protein modifier from *Saccharomyces cerevisiae*, Urm1p. Simultaneous loss of Urm1p and Cla4p, a p21-activated kinase that functions in budding, is lethal. This result suggests a role for the urmylation pathway in budding. Furthermore, loss of the urmylation pathway causes defects in invasive growth and confers sensitivity to rapamycin. Our results indicate that the sensitivity to rapamycin is due to a genetic interaction with the TOR pathway, which is important for regulation of cell growth in response to nutrients. We have found that Urm1p can be attached to a number of proteins. Loss of five genes that are also essential in a *cla4*Δ strain, *NCS2*, *NCS6*, *ELP2*, *ELP6*, and *URE2*, affect the level of at least one Urm1p conjugate. Moreover, these five genes have a role in invasive growth and display genetic interactions with the TOR pathway. In summary, our results suggest the urmylation pathway is involved in nutrient sensing and budding.

INTRODUCTION

A principal feature of morphogenesis in eukaryotes is cell polarization, which involves the asymmetric organization of the cytoskeleton and the attendant asymmetric organization of internal membranes and proteins (Drubin and Nelson, 1996). The Rho-GTPase Cdc42p plays a critical role in regulation of polarized cell growth and in the regulation of other morphogenetic events such as cytokinesis (Adams *et al*., 1990; Johnson and Pringle, 1990; Ziman *et al*., 1993; Li *et al*., 1995; Richman and Johnson, 2000). Cdc42p orchestrates these events via activation of effector proteins. For example, activated Cdc42 binds to and regulates Gic1p and Gic2p, which are important for the polarization of the actin cytoskeleton (Brown *et al*., 1997; Chen *et al*., 1997). The p21-activated kinases (PAKs) Ste20p and Cla4p (Cvrckova *et al*., 1995; Peter *et al*., 1996; Leberer *et al*., 1997) are two other Cdc42p effectors. Both Ste20p and Cla4p have poorly characterized roles in polarizing the actin cytoskeleton and in septin function but together these two PAKs are required for viability (Cvrckova *et al*., 1995).

To gain insight into the physiological events that have been perturbed in a *ste20*Δ *cla4*Δ mutant, we used a synthetic lethal mutant screen to identify additional genes that are required in the absence of Cla4p. This effort led to the identification of NCS3 (*N*eeds *C*LA4 to *S*urvive; identical to *UBA4*) and a number of other genes as well (Mitchell and Sprague, 2001; Goehring *et al*., 2003). *UBA4* encodes a protein that has 47% sequence similarity to Uba1p (amino acids 416–574), an ubiquitin-activating enzyme (E1). Uba1p forms a thioester linkage between a cysteine within Uba1p and the C-terminal glycine of ubiquitin. Ubiquitin is then transferred to another carrier protein (E2) with the formation of a new thioester linkage and eventually is covalently attached to proteins targeted for destruction. Recently, Uba4p was shown to function in a novel ubiquitin-like conjugation pathway as a protein activation enzyme (E1) of *u*biquitin *r*elated *m*odifier (Urm1p). In parallel with the ubiquitin system, Urm1p forms a thioester bond with Uba4p (Furukawa *et al*., 2000). This interaction depends on the carboxy-terminal glycine residue of Urm1p and a cysteine residue in Uba4p (Furukawa *et al*., 2000).

Ubiquitin-like proteins (Ubl) have recently been discovered in most eukaryotes, suggesting that the covalent attachment of these Ubls to target proteins is a common posttranslational modification (Hochstrasser, 2000). In contrast to ubiquitin, most of these Ubls don't seem to promote proteolysis. For example, *s*mall-*u*biquitin-related-*mo*difier (SUMO1) is required for the localization of *R*an GTPase *a*ctivating *p*rotein (RanGAP1) to the nuclear pore (Mahajan *et al*., 1997, 1998). Similarly, although *r*elated-to-*ub*iquitin (Rub1p) conjugation to the ubiquitin-ligase (Skp1p/cullin-1/F-box protein) may regulate the ubiquitin conjugation pathways (Lammer *et al*., 1998; Liakopoulos *et al*., 1998; Kawakami *et al*., 2001), this conjugation does not promote proteolysis directly. Although the target(s) or function(s) for the urmylation pathway is unknown, Urm1p seems to have a human counterpart and is suggested to fulfill a basic function in eukaryotic cells (Furukawa *et al*., 2000).

In this study, we show that the Urm1p-conjugation system in *Saccharomyces cerevisiae* plays a role in budding and haploid invasive growth. Both Uba4p and Urm1p are required in cells lacking *CLA4*. In addition, loss of either *UBA4* or *URM1* leads to a defect in invasion. Using an antibody to Urm1p, we identified several potential urmylated targets. Moreover, we found that loss of a subset of proteins, Ncs2p,

Article published online ahead of print. Mol. Biol. Cell 10.1091/mbc.E03–02–0079. Article and publication date are available at www.molbiolcell.org/cgi/doi/10.1091/mbc.E03–02–0079.

* Present address: Howard Hughes Medical Institute, Vollum Institute, Oregon Health and Science University, Portland, OR 97239.
† Corresponding author. E-mail address: gsprague@molbio.uoregon.edu.

Table 1. Yeast strains used in this study

Strain[a]	Relevant genotype	Reference
SY3357	*MAT***a** *leu2-Δ1 ura3-52 his3-Δ200 trp1-Δ63 ade8Δ ade2-101 mfa2-Δ1::FUS1-lacZ*	Mitchell and Sprague, 2001
SY3358	*MATα leu2-Δ1 ura3-52 lys2-801 his3-Δ200 trp1-Δ63 ade8Δ ade2-101 mfa2-Δ1::FUS1lacZ*	Mitchell and Sprague, 2001
SY3362	SY3357 except *cla4Δ::TRP1* (pRS316*ADE8CLA4)*	Mitchell and Sprague, 2001
SY3380	SY3357 except *cla4Δ::TRP1* (YCp*HIS3cla4-75)*	Mitchell and Sprague, 2001
SY3764	SY3357 except *cla4Δ::TRP1 ste20Δ::TRP1* (YCp*HIS3cla4-75)*	Goehring *et al.*, 2003
SY3754	SY3358 except *cla4Δ::TRP1 ste20Δ::TRP1* (pRS316*ADE8CLA4)*	This study
SY3805	SY3358 except *uba4Δ::KanMX6*	This study
SY3806	SY3358 except *urm1Δ::KanMX6*	This study
SY3807	SY3357 except *cla4Δ::TRP1 uba4Δ::HIS3* (pRS316*ADE8CLA4)*	This study
SY3808	SY3357 except *cla4Δ::TRP1 urm1Δ::KanMX6* (pRS316*ADE8CLA4)*	This study
SY3809	SY3357 except *cla4Δ::TRP1 uba4Δ::KanMX6* (YCp*HIS3cla4-75)*	This study
SY3810	SY3357 except *cla4Δ::TRP1 urm1Δ::KanMX6* (YCp*HIS3cla4-75)*	This study
SY3815	SY3358 except *ncs2Δ::KanMX6*	This study
SY3816	SY3358 except *ncs6Δ::KanMX6*	This study
SY3817	SY3358 except *elp2Δ::KanMX6*	This study
SY3818	SY3358 except *elp6Δ::KanMX6*	This study
SY3819	SY3358 except *ure2Δ::KanMX6*	This study
SY3820	SY3357 except *cla4Δ::TRP1 KanMX6* P_{GAL1}*-YNL119w* (pRS316*ADE8CLA4)*	This study
SY3821	SY3357 except *cla4Δ::TRP1 KanMX6* P_{GAL1}*-YNL120c* (pRS316*ADE8CLA4)*	This study
SY3822	SY3357 except *cla4Δ::TRP1 ncs2Δ::KanMX6* (YCp*HIS3cla4-75)*	This study
SY3823	SY3357 except *cla4Δ::TRP1 ncs6Δ::KanMX6* (YCp*HIS3cla4-75)*	This study
SY3824	SY3357 except *cla4Δ::TRP1 elp6Δ::KanMX6* (YCp*HIS3cla4-75)*	This study
SY3825	SY3357 except *cla4Δ::TRP1 ure2Δ::KanMX6* (YCp*HIS3cla4-75)*	This study
HYL333	*MATα ura3-52*	G. Fink
HYL334	*MAT***a** *ura3-52*	G. Fink
SY3826	HYL333 except *his3Δura3*	This study
SY3827	SY3826 except *uba4Δ::KanMX6*	This study
SY3828	SY3826 except *urm1Δ::KanMX6*	This study
SY3829	SY3826 except *ncs2Δ::KanMX6*	This study
SY3830	SY3826 except *ncs6Δ::KanMX6*	This study
SY3831	SY3826 except *elp2Δ::KanMX6*	This study
SY3832	SY3826 except *elp6Δ::KanMX6*	This study
SY3833	SY3826 except *ure2Δ::KanMX6*	This study
SY3834	HYL333 except *ste20Δ::URA3*	This study
SY4148	HYL333/HYL334 except *leu2ΔURA3*	This study
SY4149	SY4148 except *uba4Δ::ura3/uba4Δ::ura3*	This study
SY3835	BY4741 except *rrd1Δ::KanMX6*	This study
SY3836	BY4741 except *gln3Δ::KanMX6*	This study
SY3837	HYL333 except *ste20Δ:: URA3 urm1Δ::ura3*	This study
SY3838	HYL333 except *ste20Δ:: ura3 uba4Δ::URA3*	This study
BY4741	*MAT***a** *his3Δ1 leu2Δ0 metl5Δ0 ura3Δ0*	Research Genetics
SY3839	BY4741 *urm1Δ::KanMX4*	Research Genetics
SY3840	BY4741 *uba4Δ::KanMX4*	Research Genetics
SY3841	BY4741 *ncs2Δ::KanMX4*	Research Genetics
SY3842	BY4741 *ncs6Δ::KanMX4*	Research Genetics
SY3843	BY4741 *elp2Δ::KanMX4*	Research Genetics
SY3844	BY4741 *elp6Δ::KanMX4*	Research Genetics
SY3845	BY4741 *ure2Δ::KanMX4*	Research Genetics
SY4150	SY3845 except *gln3Δ::NatMX4*	Research Genetics
SY4151	BY4741 except *gln3Δ::KanMX4*	Research Genetics

[a] SY3357 and SY3358 are derivatives S288C.

[b] Strains containing the designation *ura3* were made *URA3* at the designated chromosomal locus and then *ura3* by selection on 5-FOA as described in MATERIALS AND METHODS.

Ncs6p, Elp6p, and Ure2p, which are essential in *cla4Δ* cells, affect the levels of at least one potential urmylated target. Loss of Ncs2p, Ncs6p, Elp2p, Elp6p, or Ure2p causes a defect in invasive growth. Ure2p has a known role in pseudohyphal growth in diploids, is a repressor of genes involved in nitrogen and glucose metabolism, and is part of a signaling cascade downstream of the Tor proteins (Cardenas *et al*., 1999; Hardwick *et al*., 1999; Kuruvilla *et al*., 2002). Together, our results suggest that the Urm1p conjugation pathway is functionally affiliated with vegetative and invasive growth and may play a regulatory role in TOR signaling.

MATERIALS AND METHODS

Strains and Growth Conditions

Yeast strains used in this study are listed in Table 1. Haploid *MAT***a** nonessential yeast deletion strains were purchased from Research Genetics (Huntsville, AL). Other gene deletions were constructed by PCR (Baudin *et al*., 1993) by using either the pRS (Sikorski and Hieter, 1989) or pFA6a (Longtine *et al*.,

Table 2. Plasmids used in this study

Plasmid	Description	Plasmid number	Reference
YCp*HIS3cla4-75*		pSL2679	Cvrckova *et al*., 1995; Mitchell and Sprague, 2001
pRS316*ADE8CLA4*		pSL2764	Mitchell and Sprague, 2001
pML40	pRS315 *TOR2*	CY3801	Lorenz and Heitman, 1995
pML41	pRS315 *TOR2-1*	CY3802	Lorenz and Heitman, 1995
CB2516	2μ *URA3 TAP42 TAP42*	PSL2826	Di Como and Arndt, 1996
P_{GAL1} pRS315	*GAL1* promoter in pRS315	pSL2775	This study
P_{GAL1} pRS315 *URM1*	*URM1* in pSL2772	pSL2776	This study
P_{GAL1} pRS315 *HFURM1*	N-terminal His6-FLAG tagged *URM1* in pSL2776	pSL2777	This study
pET *HFURM1*	N-terminal His6-FLAG tagged *URM1* in pET22b	pSL2778	This study
pMBP-*URM1*	N-terminal MBP tagged *URM1* in pMAL-c2	pSL2779	This study

1998) plasmid series as templates. In all cases, the entire coding region was replaced with the indicated marker and successful replacement was confirmed by PCR and phenotype when applicable. Yeast strains were propagated using standard methods (Rose *et al*., 1990). Rich yeast media, containing 2% glucose (YPD), and synthetic yeast media containing either 2% glucose (SCD) or 2% galactose (SCG), were prepared as described (Rose *et al*., 1990). Strains were cured of *URA3*-containing plasmids by using 5-fluoroorotic acid (5-FOA; Biovectra, CA). Geneticin (Biovectra) selection was performed as previously described (Longtine *et al*., 1998). Rapamycin (Sigma-Aldrich, St. Louis, MO) was added to the medium from a concentrated stock solution in 90% ethanol/10% Tween 20. Yeast transformations were performed as described previously (Gietz *et al*., 1995).

Identification of NCS2

Previously, we described *NCS2* as either of two overlapping open reading frames (ORFs), *YNL119w/YNL120c*. To determine whether loss of *YNL119w* or *YNL120c* was lethal in combination with a *cla4*Δ mutation, the promoter for each gene was replaced separately with a *GAL1* promoter in strain SY3358. The *GAL1* promoter was amplified by PCR by using the pFA6a-kanMX6-PGAL1 (Longtine *et al*., 1998) plasmid as a template. Growth of the resulting strains was tested on SCD or SCG supplemented with 5-FOA.

Plasmids

The plasmids used in this study are shown in Table 2. Enzymes used for DNA manipulations were purchased from New England Biolabs (Beverly, MA), or Boehringer Mannheim Biochemicals (Indianapolis, IN). Oligonucleotides were synthesized by Keystone Laboratories (Camarillo, CA). Bacterial transformations and DNA preparations were performed by standard methods (Sambrook *et al*., 1989). The P_{GAL1} pRS315 plasmid was created using homologous recombination to replace the *URA3* gene of P_{GAL1} pRS316 with *LEU2* (Ma *et al*., 1987; Baudin *et al*., 1993). The plasmid for P_{GAL1}-driven expression of Urm1p was produced by inserting polymerase chain reaction (PCR)-derived fragments from yeast genomic *URM1* DNA by using *Taq* polymerase (Promega, Madison, WI) and the oligonucleotides 5′-GCCCG**GGATCC**GATGGTAAA CGTGAAAGTGGAG-3′ (incorporating a *Bam*HI site shown in bold type) and 5′-CTCGAGT**GCGGCCGC**CTGCTATTTTTAACCACCATG-3′ (incorporating a *Not*I site shown in bold type; sequence corresponding to *URM1* is underlined). This 300-base pair PCR product was cloned into *Bam*HI- and *Not*I-digested P_{GAL1}pRS315 (pSL2775), thus creating P_{GAL1}-pRS315 *URM1*. The P_{GAL1}-driven *URM1* construct that bears the N-terminal extension MT-SHHHHHHMHDYKDDDDKMGS containing His6- and FLAG-tags was generated by inserting PCR-derived fragments into *Bam*HI- and *Not*I-digested P_{GAL1} pRS315 (pSL2775). The His6-FLAG *URM1* fragments were created by a two-step PCR. The first round of PCR generated FLAG *URM1* by using the oligonucleotides 5′-CATGCACGATTACAAG*GATGACGACGATAAG*ATGGGGTCGATGGTAA ACGTGAAAGTGGAG (FLAG tag shown in italics; sequence corresponding to *URM1* is underlined) and 5′-CTCGAGT**GCGGCCGC**CTGCTATT TTTAACCACCATG-3′ (incorporating a *Not*I site, shown in bold type; sequence corresponding to *URM1* is underlined). To generate His6-FLAG *URM1*, the FLAG *URM1* PCR product was used as a template in a reaction with the oligonucleotides 5′-GCCCGGGATCCGCATATGA CCTCG*CATCATCACCACCATCAC*ATGCACGATTACAAGGATGAC (incorporating a *Bam*HI site and a *Nde*I site, both shown in bold type; His6 tag, shown in italics) and 5′-CTCGAGT**GCGGCCGC**CTGCTATTTTTAACCACCATG-3′ (incorporating a *Not*I site, shown in bold type; sequence corresponding to *URM1* is underlined). This PCR product was digested with *Bam*HI and *Not*I and inserted into *Bam*HI and *Not*I digested P_{GAL1}-PRS315, thus creating P_{GAL1}-PRS315 *HFURM1.* pET-*HFURM1* is a pET-22b-derived plasmid (Novagen, Madison, WI) that was generated by digest of P_{GAL1}-PRS315 *HFURM1* with *Nde*I and *Not*I and followed by insertion into pET-22b. pMBP-*URM1* is a pMAL-c2 (New England Biolabs) derived plasmid that was created by subcloning the *Bam*HI/*Not*I digested PCR product generated by oligonucleotides 5′-GCC**GGATCC**ATGGTAAACGTGA AAGTGGAG-3′ (incorporating a *Bam*HI site, shown in bold type) and 5′-GAGCTCTA A**CTGCAG**GGTAGTACCCGGTAGCCCTTC-3′ (incorporating a *Pst*I site, shown in bold type) into pMAL-c2. The other plasmids used in this study, YCp*HIS3cla4-75*, pML40, pML41, pRS316*ADE8CLA4*, and 2 μ *URA3 TAP42* (CB2516) have been described previously (Cvrckova *et al*., 1995; Lorenz and Heitman, 1995; Di Como and Arndt, 1996; Mitchell and Sprague, 2001).

Antibodies

A rabbit polyclonal antibody was raised against His6-FLAG-Urm1p and was affinity purified on a MBP-Urm1p affinity column (Harlow and Lane, 1988). To create the MBP-Urm1p affinity column, 10 ml of a saturated culture of *Escherichia coli* BL21(DE3) carrying pSL2779 was diluted into 1 liter of LBH supplemented with 0.2% glucose and 50 μg/ml ampicillin, grown at 37°C to an OD_{600} of 0.6, supplemented with isopropyl-1-thio-B-D-galactopyranoside to 0.3 mM, and incubated at 37°C for another 3 h. Cells were harvested by centrifugation, resuspended in 50 ml of lysis buffer (20 mM Tris pH 7, 200 mM NaCl, 1 mM EDTA), and lysed by French press. Lysates were clarified by centrifugation at 12,000 $\times$ *g*, diluted with 250 ml of lysis buffer, loaded onto 5 ml of amylose resin (New England Biolabs, Beverly, MA), washed with lysis buffer, and maltose binding protein eluted with lysis buffer supplemented with 100 mM maltose. The eluate was dialyzed against 25 mM HEPES pH 7.5 (Sigma-Aldrich) and then 35 mg of MBP-Urm1p was coupled to 1 ml of Affi-gel-15 (Bio-Rad, Hercules, CA) according to the manufacturer's instructions. In a whole cell lysate from a *uba4*Δ mutant, the affinity-purified anti-Urm1p antibody recognized free unconjugated Urm1p, as well as a many other bands unrelated to Urm1p (our unpublished observations). Therefore, the antibody was further purified by incubation with an acetone pellet of a *urm1*Δ mutant strain (SY3805) as described previously (Harlow and Lane, 1988) with a few modifications. Before the addition of acetone, the cells were incubated with zymolyase (~1 mg/1000 ODs; Seikagaku America, Ijamsville, MD) for 20 min at 30°C. After acetone precipitation, the powder was added to the sera at a concentration of 10 mg/ml, incubated overnight at 4°C, and then removed by centrifugation. After the second purification of the anti-Urm1p antibody, the antibody recognized free unconjugated Urm1p, as well as five bands (~131, 65, 55, 50, and 41 kDa) unrelated to Urm1p in a whole cell lysate of a *uba4*Δ mutant (Figure 2, lane 2).

A rabbit polyclonal antibody against Cdc3p, a generous gift of J. Pringle (University of North Carolina, Chapel Hill, NC) was affinity purified on a nitrocellulose filter containing MalE-Cdc3p as described previously (Kim *et al*., 1991).

Microscopy

Indirect immunofluorescence was performed essentially as described previously (Goehring *et al*., 2003) to visualize the septins by using an α-Cdc3p antibody. For indirect immunofluorescence of Urm1p, cells were grown in YEPD at 30°C to 1 OD_{600}/ml, fixed by the addition of 3% formaldehyde for 1 h, and incubated for 16 h at room temperature in 4% paraformaldehyde, 50 mM KPO_4 pH 6.5. Cells were converted to spheroplasts by using zymolyase 100T, permeabilized by treatment with 5% SDS for 5 min, and adhered to poly(L-lysine) multiwell-coated slides. Nonspecific antibody binding was blocked by incubation of the cells in phosphate-buffered saline containing 5 mg/ml bovine serum albumin. All antibodies were diluted in phosphate-buffered saline with 5 mg/ml bovine serum albumin, which was also used for all washes. Antibodies against Urm1p were preabsorbed to yeast proteins (to remove nonspecific binding) by incubation with *urm1*Δ cells. Antibody incu-

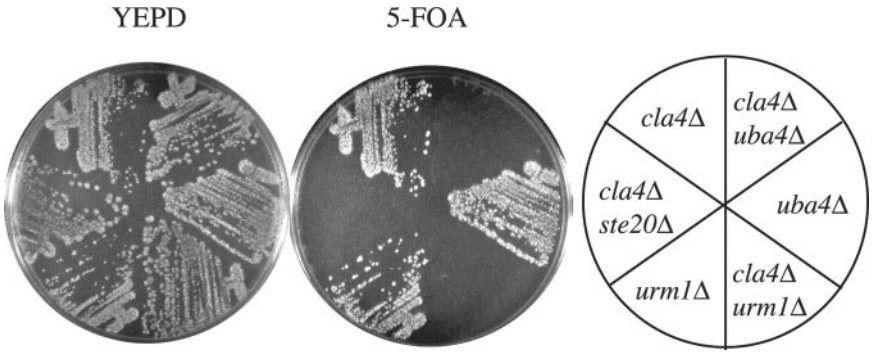

Figure 1. Loss of Urm1p and Uba4p is synthetically lethal with *cla4*Δ. Strains SY3362 (*cla4*Δ), SY3805 (*uba4*Δ), SY3806 (*urm1*Δ), SY3807 (*uba4*Δ *cla4*Δ), SY3808 (*urm1*Δ *cla4*Δ), and SY3754 (*ste20*Δ *cla4*Δ) harboring pRS316*ADE8CLA4* were streaked on YEPD plates and incubated at 30°C for 2 d. Plates were then replica-plated to 5-FOA and incubated at 30°C for 3 d.

bations were performed at room temperature for 1 h. Alexa (A594)-conjugated goat anti-rabbit antibodies were obtained from Molecular Probes. Images were generated by using an Axioplan 2 fluorescence microscope (Carl Zeiss, Thornwood, NY) fitted with an Orca 100 digital camera (Hamamatsu, Bridgewater, NJ). All assays were performed in triplicate.

Invasive and Pseudohyphal Growth Assays

For the plate-washing invasive growth assay, strains were patched on YPD plates and incubated at 30°C. After 2 d of incubation (unless otherwise indicated), plates were washed under a stream of running water as the surface was gently rubbed with a finger to remove cells not in the agar, and invasive growth was scored (Roberts and Fink, 1994). The single cell invasive growth assay was performed as described previously (Cullen and Sprague, 2000). Cells were grown to stationary phase in synthetic medium, washed twice with water, and plated onto fresh synthetic medium lacking glucose (SC) at a concentration of 10^4 cells/plate. The plates were incubated at 25°C for 12 h. Cells were scraped from plates by using 4 ml of distilled water, concentrated by centrifugation, resuspended in 20 μl of water and assayed by microscopy for the formation of the filamentous form. All assays were performed in triplicate. For the pseudohypal growth assay cells were plated to SLAD medium, grown for 3 d at 30°C, followed by microscopic examination of pseudohypal formation (Gimeno *et al*., 1992).

Immunoblot Analysis of Whole Yeast Lysates

Yeast strains were grown to mid-exponential phase (OD_{600} ~0.8) in YPD at 30°C. Culture aliquots containing equal numbers of cells, determined by OD_{600}, were collected by centrifugation, washed once in water, and the yeast pellet was frozen. The pellet was resuspended in buffer A (50 mM Tris pH 8.0, 1% NP-40, 50 mM NaCl, 1 mM EDTA) containing a mixture of protease inhibitors (1 mM phenylmethylsulfonyl fluoride, 1 μg/ml leupeptin, 1 μg/ml pepstatin A, 1 μg/ml aprotinin [all from Sigma-Aldrich], and 1 tablet of protease inhibitor mixture Complete/25 ml [Roche Diagnostics, Indianapolis, IN]). The lysis buffer also contained 20 mM *N*-ethylmaleimide (NEM; Sigma-Aldrich) unless otherwise noted. The cells were broken by vortexing with glass beads, and the resulting extracts were centrifuged at 2000 × *g* to remove glass beads and unbroken cells. SDS- and dithiothreitol-containing loading buffer was added to the extracts, which were loaded onto 10% SDS-PAGE, subjected to electrophoresis, and electroblotted to nitrocellulose. Urm1p was detected using polyclonal antibody to Urm1p, a secondary anti-rabbit horseradish peroxidase-conjugated antibody (Bio-Rad), and chemiluminescence (Pierce Chemical, Rockford, IL). A monoclonal antibody against Dpm1p (a kind gift from T. Stevens, University of Oregon, Eugene, OR) and a secondary anti-mouse horseradish peroxidase-conjugated antibody (Bio-Rad) were used to confirm that equal amounts of protein were loaded in each lane.

RESULTS

The Urmylation Pathway Is Essential in cla4Δ Cells

Previously, we identified Uba4p in a screen for proteins that were essential in a *cla4*Δ mutant (Goehring *et al*., 2003). Because Urm1p had been shown to form a thioester linkage with Uba4p (Furukawa *et al*., 2000), we tested whether the loss of Urm1p was essential in a *cla4*Δ background. Like *uba4* mutations, mutations in *URM1* were synthetically lethal with *cla4*Δ (Figure 1).

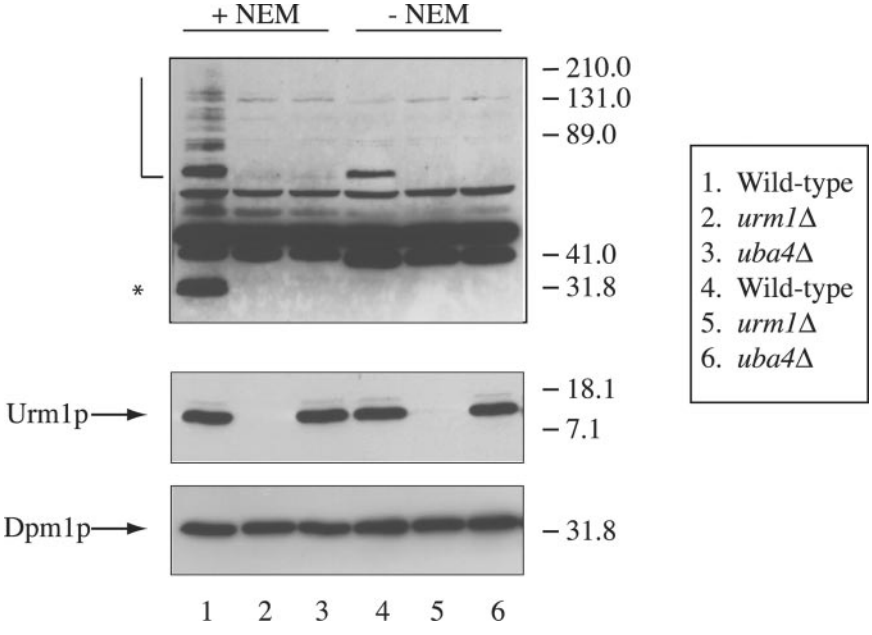

Figure 2. Immunoblot analysis with anti-Urm1p antibodies. Exponential cultures of haploid strains SY3358 (WT), SY3806 (*urm1*Δ) and SY3805 (*uba4*Δ), were lysed in the presence of 20 mM NEM (lanes 1–3) or in the absence of NEM (lanes 4–6). Lysates were analyzed by SDS-PAGE and immunoblot analysis by using affinity-purified polyclonal anti-Urm1p antibodies and monoclonal antibodies to Dpm1p (to confirm equal protein loading). The band corresponding to unconjugated Urm1p is indicated. A half-open square bracket designates high molecular mass Urm1p modified species, whereas an asterisk denotes the position of a 32-kDa Urm1p-modified species.

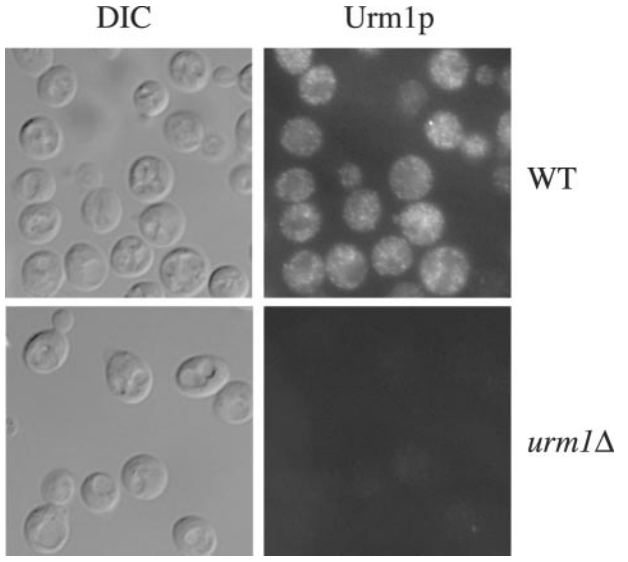

Figure 3. Immunolocalization of Urm1p. Immunofluorescence microscopy of strains SY3358 (WT) and SY3806 (*urm1*Δ) by using a polyclonal antibody against Urm1p. Cells were also visualized by differential interference contrast.

Identification of Potential Urmylated Products

To detect free Urm1p and possible Urm1p-protein conjugates, we generated polyclonal antibodies to Urm1p (see MATERIALS AND METHODS). One difficulty in identifying targets of the ubiquitin-like modifiers has been that these proteins are rapidly deconjugated by isopepetidases upon cell lysis in nondenaturing buffers (Li and Hochstrasser, 2000). We therefore prepared lysates with and without NEM, an isopeptidase inhibitor. In Western analysis with the polyclonal Urm1p antibody, lysates prepared either in the presence or absence of NEM contained a polypeptide of ~13 kDa (free Urm1p; Figure 2, lanes 1, 3, 4, and 6) and a polypeptide ~75 kDa, although the latter was less abundant in the absence of NEM (Figure 2, lane 3). Intriguingly, Urm1p itself may undergo posttranslational modification because it forms as a doublet (Figure 2, lanes 1, 3, 4, and 6). In the presence of NEM, the Urm1p antibody also recognized an ~32-kDa protein and many other polypeptides of higher molecular weight. Each of these bands presumably represents an urmylated protein because they are not detected in extracts of *urm1*Δ or *uba4*Δ cells.

To determine the intracellular localization of Urm1p and the urmylated products, we used the antibody to Urm1p. Urm1p seemed to localize to the cytoplasm and to punctuate spots within the cytoplasm (Figure 3). To gain additional information about the location of Urm1p and the possible Urm1p-protein conjugates, wild-type and *uba4*Δ cell lysates were fractionated by centrifugation into a 13,000 × *g* (P13), a 100,000 × *g* pellet (P100), and a 1000,000 × *g* supernatant solution (S100). Essentially all of the Urm1p and Urm1p-protein conjugates were found in the cytosol (our unpublished observations).

Loss of Ncs2, Ncs6p, Elp2, Elp6p, and Ure2p Affects the Presence of Potential Urmylated Products

Previously, we identified a large number of proteins that were essential in a *cla4*Δ mutant (Goehring *et al*., 2003). To determine whether any of these proteins are components or targets of the urmylation pathway, we performed Western analysis with the anti-Urm1p antibody on strains lacking all 65 genes identified as *NCS*s. Except for *UBA4*, loss of the identified *NCS* genes did not completely eliminate any of the potential urmylated targets (our unpublished observations). However, loss of four genes (*NCS2*, *NCS6*, *ELP6*, and *ELP2*) did decrease the abundance of the ~75-, 80-, 89-, and 125-kDa polypeptides (Figure 4A, lanes 4–7, respectively). Elp2p and Elp6p are components of the elongator RNA polymerase II holoenzyme. They stimulate the transcription elongation and are important for normal histone acytelation levels (Fellows *et al*., 2000; Krogan and Greenblatt, 2001; Winkler *et al*., 2001, 2002). *NCS6* is an open reading frame (ORF), *YGL211w*, encoding for a protein of unknown function; it has homology to other proteins, also of unknown function (Goehring *et al*., 2003). *NCS2* was identified as one of two overlapping, uncharacterized ORFs, *YNL119w* or *YNL120c* (Goehring *et al*., 2003; Figure 5A). To identify the bona fide *NCS2* gene, a *GAL1* promoter was inserted in place of the promoter for each ORF and the resulting constructs introduced into a *cla4*Δ mutant strain. On medium containing 5-FOA and glucose (SCD + 5-FOA), neither P_{GAL1}*YNL119w cla4*Δ nor P_{GAL1}*YNL120c cla4*Δ was able to survive. Only *GAL1*-driven expression of *YNL119w* allowed for growth on 5-FOA galactose media (Figure 5B), indicating that *YNL119w* is *NCS2*.

Loss of a fifth gene, *URE2*, did not affect the ~75-, 80-, 89-, and 125-kDa polypeptides, but instead, in this mutant background, a new band recognized by the Urm1p antibody occurred at ~131 kDa (Figure 4A, lane 8). *URE2* encodes for a protein that is part of a signaling cascade downstream of the TOR proteins and is a transcriptional repressor for genes involved in nitrogen and glucose signaling (Cardenas *et al*., 1999; Hardwick *et al*., 1999; Kuruvilla *et al*., 2002). Both Ure2p and the TOR pathway function in diploids to promote the transition from a vegetative form to a pseudohyphal form in response to nutrient limitations. One protein regulated by Ure2p is Gln3p, a GATA-type transcription factor that functions downstream of the TOR kinases to regulate the expression of genes involved in nutrient sensing (Beck and Hall, 1999; Bertram *et al*., 2000; Rempola *et al*., 2000). To determine whether Gln3p also affects the presence of urmylated products, we tested whether the 131-kDa band recognized by the Urm1p antibody is present in a *gln3*Δ ure2Δ mutant. We found that in the absence of Gln3p, the 131-kDa product was not detected (Figure 4B), suggesting that the urmylation of this protein requires Gln3p.

Urmylation Pathway Has a Role in Invasive and Pseudohyphal Growth

When haploid cells are starved for nutrients, the cells undergo a switch from a vegetative form to a filamentous form. During vegetative growth, the cells are round and bud in an axial manner (buds are formed adjacent to the previous bud site). When nutrients are limiting, the cells become elongated, bud primarily from one pole, and can invade the agar substratum. Because Ste20p was shown to have a role in invasive growth and, like the urmylation pathway components, is essential in a *cla4*Δ mutant background, we tested to see whether loss of the urmylation pathway components and the genes that affect the potential Urm1p-protein conjugates cause a defect in invasion. Loss of *UBA4*, *URM1*, *ELP2*, *ELP6*, *NCS2*, and *NCS6* renders cells unable to invade agar under starvation conditions (Figure 6A). To investigate whether loss of these

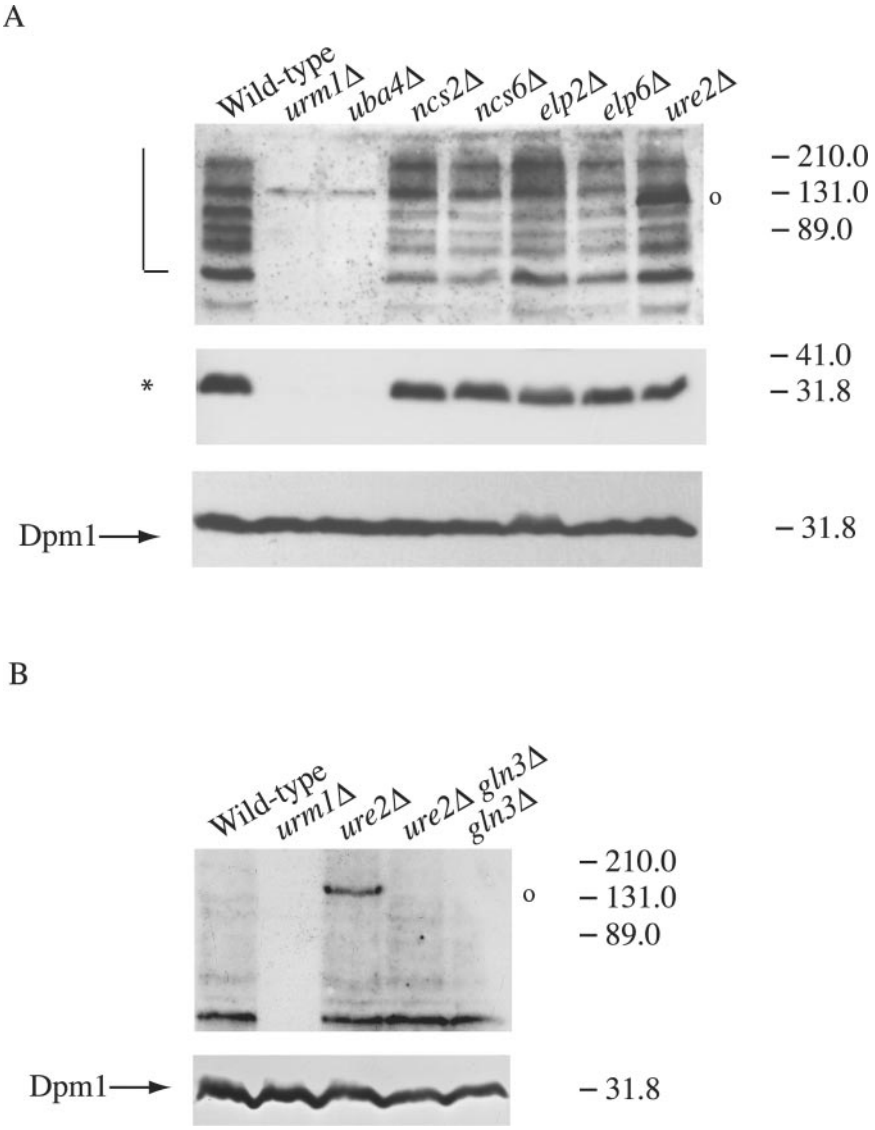

Figure 4. Loss of Ncs2p, Ncs6p, Elp2p, Elp6p, and Ure2p alter the pattern of Urm1p-conjugates. (A) Strains SY3358 (wild-type) SY3806 (*urm1*Δ), SY3805 (*uba4*Δ), SY3815 (*ncs2*Δ), SY3816 (*ncs6*Δ), SY3817 (*elp2*Δ), SY3818 (*elp6*Δ), and SY3819 (*ure2*Δ) were grown to mid-log in YEPD at 30°C. Lysates were analyzed by SDS-PAGE and immunoblot analysis by using affinity-purified polyclonal anti-Urm1p antibodies and monoclonal antibodies to Dpm1p (to confirm equal protein loading). A half-open square bracket designates high molecular mass Urm1p-modified species, whereas an asterisk designates the positions of a 32-kDa Urm1p-modified species. A 131-kDa Urm1p-modified species that occurs in a *ure2*Δ is indicated with an open circle. (B) Urm1p immunoblot analysis was performed on strains BY4741 (wild-type) SY3839 (*urm1*Δ), SY3845 (*ure2*Δ), SY4150 (*ure2*Δ *gln3*Δ), and SY4151 (*gln3*Δ) as in part A with the exception that the immunoblots were exposed for a shorter time.

genes causes defects in other aspects of invasive growth (change in bud pattern and formation of elongated cells), we used the single cell invasive growth assay (Cullen and Sprague, 2000). This assay takes advantage of the fact that cells undergo invasive growth in response to glucose depletion. As previously reported, *ste20* mutants had a defect in bud pattern (unipolar budding) and in cell elongation by using this assay (Cullen and Sprague, 2000). We found that *uba4*Δ, *urm1*Δ, *elp2*Δ, *elp6*Δ, *ncs2*Δ, and *ncs6*Δ mutants had a defect in cell elongation, but not bud pattern, in response to glucose depletion (Figure 6B). However, *ure2*Δ mutants not only had a defect in elongation but also had a defect in bud pattern.

We next asked whether the urmylation pathway has a role in pseudohyphal development by diploid cells. We found that *uba4*Δ/*uba4*Δ mutants failed to form pseudohypae under nitrogen limiting conditions (Figure 7A). Hence, we conclude that the urmylation pathway and the other proteins affecting urmylation have a role in both haploid invasive growth and in diploid pseudohyphal development.

Ste20p and the Urmylation Pathway May Function in Parallel Pathways during Invasive Growth

Previously, it has been shown that there are several pathways that contribute to invasive growth, one of which includes Ste20p. As shown above, the urmylation pathway also seems to play a role in invasive growth. By using the single cell assay, we showed that *ste20*Δ mutants have a defect in both bud pattern and in cell elongation, whereas *urm1*Δ mutants only have a defect in cell elongation (Figure 6). To determine whether the urmylation pathway is functioning with Ste20p in invasive growth, we compared the phenotype of the double mutants to that of the single mutants. We found *ste20*Δ *urm1*Δ and *ste20*Δ *ncs3*Δ double mutants have a more severe invasive growth defect than either single mutant (Figure 8). One interpretation of these results is that *URM1* and *STE20* function independently in the invasive growth program. Alternatively, *URM1* and *STE20* may have overlapping roles in orchestration of invasive growth, for example, sharing a role in cell elongation but having distinct roles as well.

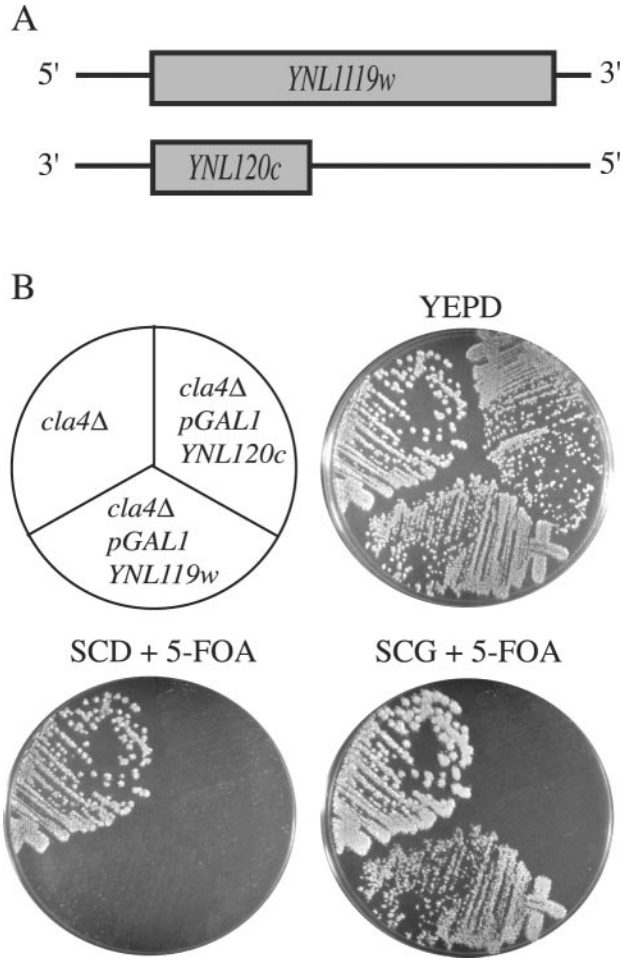

Figure 5. Identification of *NCS2* as *YNL119w*. (A) A small yeast ORF of unknown function, *YNL120c*, overlaps *YNL119w* on the other DNA strand. (B) Strains SY3362 (*cla4*Δ), SY3820 (P_{GAL1}-*YNL119w cla4*Δ), and SY3821 (P_{GAL1}-*YNL120c cla4*Δ) harboring pRS316*ADE8CLA4* were streaked on YEPD plates and incubated at 30°C for 2 d. Plates were then replica-plated to SCD + 5-FOA or SCG + 5-FOA and incubated at 30°C for 3 d.

The Urmylation Pathway Is Implicated in TOR Pathway Signaling

As this work was ongoing, another group completed a large-scale genome-wide screen and identified *ure2*Δ, *ncs6*Δ, and *uba4*Δ mutants as being hypersensitive to rapamycin, a macrocyclic antibiotic (Chan *et al*., 2000). Rapamycin inhibits Tor1p and Tor2p, ultimately resulting in cellular responses characteristic of nutrient deprivation through a mechanism involving translational and transcriptional arrest (Kunz *et al*., 1993; Helliwell *et al*., 1994; Barbet *et al*., 1996; Komeili *et al*., 2000) (see model in Figure 9C). Moreover, the TOR proteins have been shown to directly modulate a glucose sensitive signaling pathway (Hardwick *et al*., 1999), suggesting that the TOR pathway may regulate invasive growth. Although *URM1*, *ELP2*, *ELP6*, and *NCS2* were not identified in screens for TOR pathway mutants, they could have been missed because an incomplete set of gene deletion strains was used for the analysis. We therefore tested whether loss of these genes conferred sensitivity to rapamycin and whether the mutations exhibited genetic interaction with TOR pathway mutations. A *rrd1*Δ/*ncs1*Δ mutant, which is defective for a protein phosphatase type 2A essential in *cla4*Δ cells, and a *gln3*Δ mutant, which is defective for a GATA-type transcription factor regulated by the TOR kinases and by the Ure2p repressor (Beck and Hall, 1999; Bertram *et al*., 2000; Rempola *et al*., 2000; Mitchell and Sprague, 2001), served as rapamycin-resistant control strains. A *ure2*Δ mutant served as a control for rapamycin sensitivity. We found that null mutants lacking *URM1*, *ELP2*, *ELP6*, or *NCS2* were unable to grow after 5 d on medium containing rapamycin (Figure 9A). Furthermore, loss of the urmylation pathway, or *ELP2*, *ELP6*, *NCS2*, or *NCS6*, conferred greater sensitivity to rapamycin than did loss of *URE2*. None of the mutants was sensitive to cycloheximide, suggesting that sensitivity to rapamycin did not reflect general drug sensitivity and was not due to a reduction of protein synthesis (Figure 9A).

To verify that the sensitivity of these mutants to rapamycin reflected inactivity of the TOR pathway, we measured the rapamycin sensitivity of *urm1*Δ, *elp2*Δ, *elp6*Δ, and *ncs2*Δ, mutants carrying a plasmid borne *TOR2S1972I* (*TOR2-1*) allele (Lorenz and Heitman, 1995). This allele of *TOR2* has previously been shown to confer rapamycin resistance to many sensitive mutants. We found that all the double mutants were no longer sensitive to rapamycin (Figure 9B). In contrast, the *urm1*Δ, *elp2*Δ, *elp6*Δ, or *ncs2*Δ mutants carrying a wild-type version of *TOR2* on a plasmid were still sensitive to rapamycin (our unpublished observations). These results suggest that mutants defective for the urmylation pathway are hypersensitive to rapamycin because TOR pathway signaling is abrogated.

We also investigated the relationship between the TOR and urmylation pathways in diploid pseudohyphal development. Previous studies have shown that overexpression of *TAP42*, which encodes a protein phosphatase, exacerbates pseudohypal filament formation in wild-type diploids. However, we observed that *uba4*Δ/*uba4*Δ homozygous diploids overexpressing *TAP42* failed to form filaments (Figure 7B). This result further implicates the urmylation pathway in diploid pseudohyphal growth and suggests that the pathway acts downstream of the Tap42p phosphatase.

Terminal Phenotype of Cells lacking Ncs2p, Ncs6p, Elp6p, and Ure2p in a cla4Δ Mutant Strain

Previously, the *ste20*Δ cla4Δ YCp*HIS3cla4-75* mutants were shown to have a terminal phenotype that included a failure to maintain the septin ring at the bud neck (Cvrckova *et al*., 1995). We therefore examined septin localization in *urm1*Δ *cla4*Δ YCp*HIS3cla4-75* and in *uba4*Δ *cla4*Δ YCp*HIS3cla4-75* double mutants. The phenotype of *urm1*Δ *cla4*Δ YCp*HIS3cla4-75* and *uba4*Δ *cla4*Δ YCp*HIS3cla4-75* mutants at the restrictive temperature resembled that of *ste20*Δ *cla4*Δ YCp*HIS3cla4-75* mutants: the cells were elongated with mislocalized septins (Figure 10). To test further the phenotypic parallels between *urm1*Δ *cla4*Δ and *cla4*Δ strains lacking *ELP2*, *ELP6*, *NCS2*, *NCS6*, and *URE2*, we compared the terminal phenotypes of the double mutants carrying a plasmidborne thermosensitive allele of *CLA4* (YCp*HIS3cla4-75*). We found that the loss of *ELP2*, *ELP6*, *NCS2*, or *NCS6* in a *cla4*Δ mutant conferred a terminal phenotype indistinguishable from the loss of the urmylation components in a *cla4*Δ mutant (Figure 10). However, loss of *URE2* in a *cla4*Δ strain did not result in a defect in septin ring localization. *ure2*Δ *cla4*Δ YCp*HIS3cla4-75* cells arrest with elongated buds in which the septin ring is localized normally at the mother-bud junction.

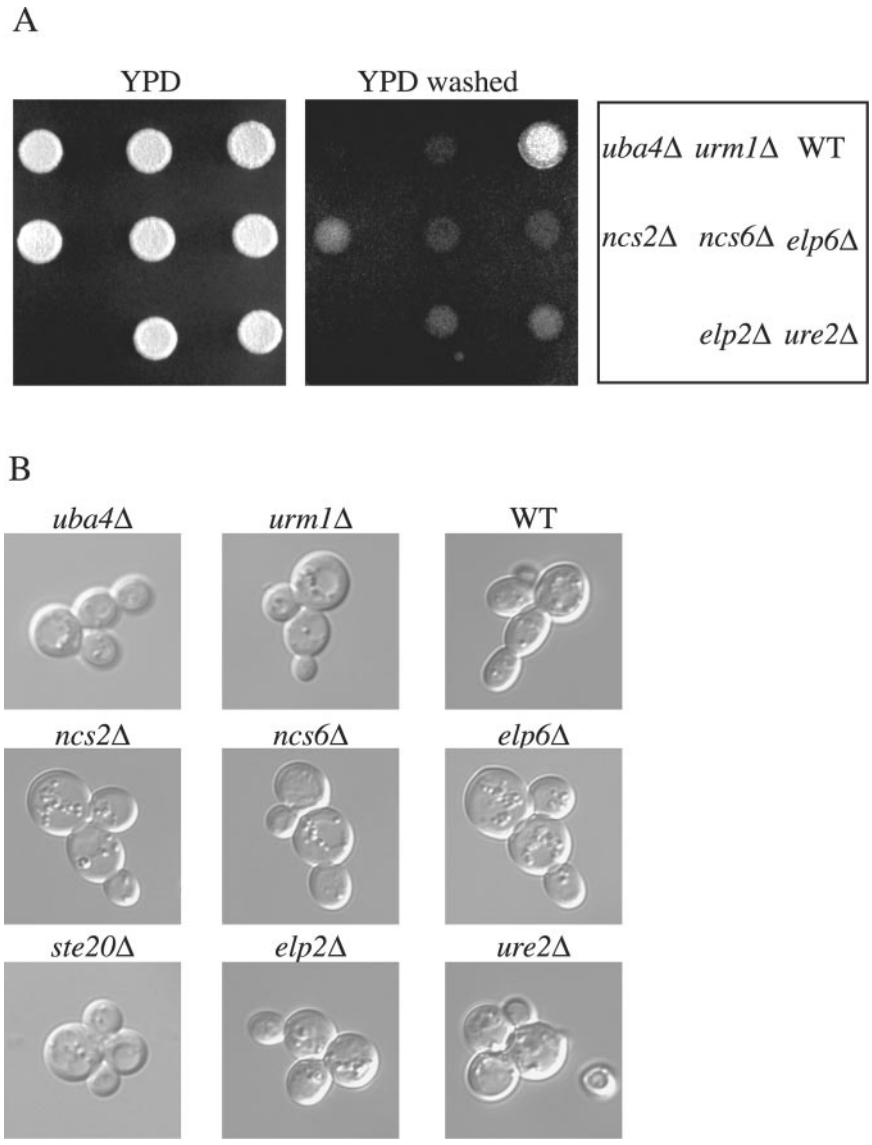

Figure 6. Role of the urmylation pathway in invasive growth. (A) Equal concentrations of strains SY3826 (WT), SY3828 (*urm1*Δ), SY3827 (*uba4*Δ), SY3832 (*elp6*Δ), SY3830 (*ncs6*Δ), SY3829 (*ncs2*Δ), SY3833 (*ure2*Δ), and SY3831 (*elp2*Δ) were spotted on YEPD plates and incubated at 30°C for 2 d. Plates were photographed, washed, and then photographed again. (B) Equal concentrations of strains SY3826 (WT), SY3828 (*urm1*Δ), SY3827 (*uba4*Δ), SY3832 (*elp6*Δ), SY3830 (*ncs6*Δ), SY3829 (*ncs2*Δ), SY3833 (*ure2*Δ), and SY3831 (*elp2*Δ) were spread onto SC medium, incubated for 16 h at 25°C, and photographed.

In previous studies, we showed that loss of Swe1p, a protein tyrosine kinase that regulates Cdc28p, can suppress some facets of the synthetic lethal phenotype exhibited by *ncs cla4* double mutants. In particular, *swe1*Δ suppressed completely the lethality of *ncs1*Δ *cla4*Δ double mutants, suppressed weakly the lethal phenotype of *uba4*Δ *cla4*Δ, *ncs6*Δ *cla4*Δ, and *elp2*Δ *cla4*Δ double mutants and did not suppress at all the lethal phenotype of the remaining *NCS* genes that were tested, including *ste20*, *bud6*, and *bni1*. We have extended this analysis and shown that *swe1*Δ also suppresses weakly the lethal phenotype of *urm1*Δ *cla4*Δ double mutants. Hence, the subgroup of *NCS* genes that affect the urmylation pattern also share this genetic suppression phenotype.

DISCUSSION

In this study, we identified roles for the urmylation pathway in both vegetative and invasive growth. Components of this novel ubiquitin-like pathway, Ncs3p/Uba4p and Urm1p, are essential in a *cla4*Δ mutant. The simultaneous loss of Cla4p and urmylation pathway components cause cells to arrest with a severe defect in budding, and we therefore suggest that the urmylation pathway has a role in vegetative growth. Using an antibody to the modifier protein, Urm1p, we identified several potential urmylated targets. Moreover, we found that loss of a subset of proteins that is essential in *cla4*Δ-Ncs2p, Ncs6p, Elp2p, Elp6p, and Ure2p, affects the level of at least one potential urmylated target. In addition to its role in vegetative growth, we found the urmylation pathway plays a role in both haploid invasive growth and diploid pseudohyphal development. Finally, loss of the urmylation pathway, as well as Ncs2p, Ncs6p, Elp2p, Elp6p, and Ure2p, causes cells to be sensitive to rapamycin suggesting a connection between these proteins and the TOR pathway. These results identify the first process in which urmylation and other proteins that affect the urmylation pathway play a role.

Urmylation of Targets

The identity of the Urm1p conjugates remains to be determined. The pattern of Urm1p conjugates is consistent with

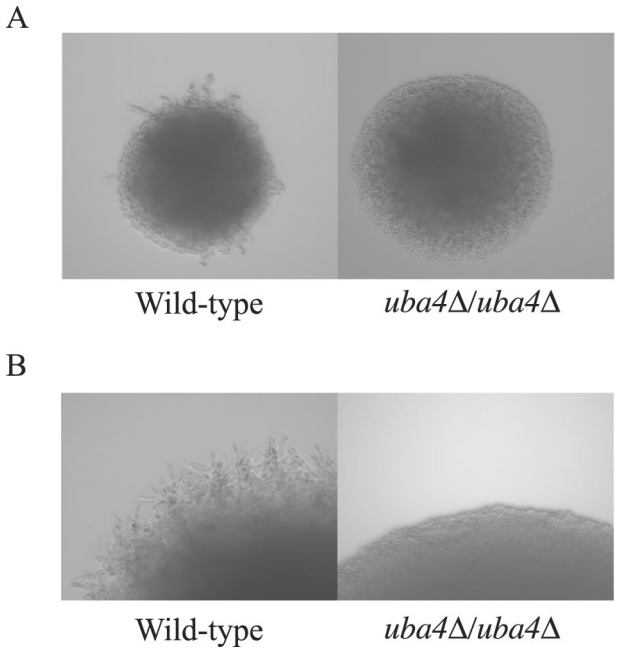

Figure 7. *UBA4* is required for diploid pseudohypal development. (A) Wild-type (SY4148) and *uba4*Δ/*uba4*Δ (SY4149) diploids were plated to SLAD medium for 3 d at 30°C. Colonies were then visualized with a 20× objective for pseudohypal formation. (B) Wild-type (SY4148) and *uba4*Δ/*uba4*Δ (SY4149) diploids containing the *TAP42* high copy plasmid (CB2516) were plated to SLAD medium for 3 d at 30 degrees. Colonies were then visualized with a 20× objective for pseudohypal filament formation.

Urm1p being attached to at least seven distinct proteins in the molecular mass range of 62–122 kDa. The most prominent band was at ~32 kDa, suggesting a substrate of ~19 kDa. A second major band at ~75 kDa suggests a substrate of ~62 kDa. We tested deletion mutants of each *NCS* gene for the presence of these urmylated products. In no case did one of the bands disappear, implying that none of these urmylated proteins corresponds to the product of an *NCS* gene.

In addition to modifying other proteins, Urm1p might itself be posttranslationally modified. When immunoblot analysis was performed on wild-type lysates, Urm1p occurs as a doublet (Figure 2, lanes 1, 3, 4, and 6), but only a small amount of the higher molecular mass band is detected, suggesting that only a fraction Urm1p is modified. Another ubiquitin-like protein, Apg12p also seems to be modified: Apg12 was shown to be conjugated to phosphatidylethanolamine thorough an amide bond between the C-terminal glycine and the amino group of phosphatidyletanolamine (Ichimura *et al*., 2000). This lipidation event is mediated by a ubiquitin-like system required for autophagy. However, the Urm1p modification does not does not require Uba4p (Figure 2, lane 3) and hence is not analogous to the Apg12p modification.

The majority of Urm1p seems to be unconjuagted. This observation is similar to ubiquitin, where 20–70% is found unconjugated (Haas and Bright, 1988; Haas *et al*., 1988) but is in contrast to Smt3p/SUMO where very little protein is unconjugated (Johnson *et al*., 1997).

Interaction of Elp2p, Elp6p, Ncs2p, Ncs6p, and Ure2p with the Urmylation Pathway

Loss of Elp2p, Elp6p, Ncs2p, and Ncs6p caused a decrease in the amount of the higher molecular mass urmylated products. Presumably this decrease reflects less urmylation rather than a reduction in the amount of these proteins, but this presumption cannot be tested until the identity of the proteins is known. The biochemical functions of Ncs2p and Ncs6p are unknown. Elp2p and Elp6p are components of a RNA polymerase II elongator complex important for the regulated expression of a subset of genes (Krogan and Greenblatt, 2001). The reduced urmylation observed in these mutants could be due to a decrease in the synthesis of urmylation enzymes or targets. Alternatively, loss of Elp2p, Elp6p, Ncs2p, and Ncs6p could affect the localization of the enzymes or targets. It is tempting to suggest that the loss of these genes is synthetically lethal with *cla4*Δ because of the decrease in abundance of the Urm1p conjugates. Identification of these products will help clarify why loss of these genes is lethal in combination with *cla4*Δ.

The pattern of Urm1p conjugates in an *ure2*Δ mutant was distinct from that in *ncs2*Δ, *ncs6*Δ, *elp2*Δ, and *elp6*Δ mutants. First, the abundance of the 32-kDa and 75- to 210-kDa conjugates did not change. More strikingly, a new conjugate (131 kDa) was detected. Ure2p is known to regulate transcription of genes involved in nitrogen and glucose signaling (Cardenas *et al*., 1999; Hardwick *et al*., 1999; Kuruvilla *et al*., 2002). It is possible that this 131-kDa gene product is

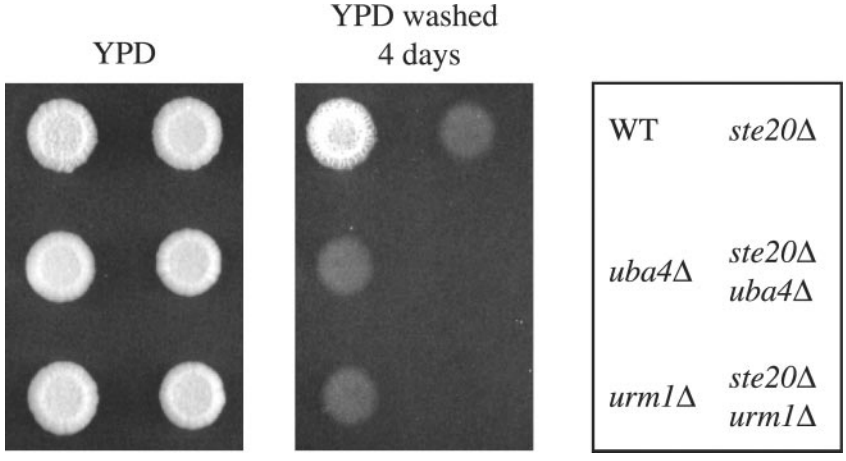

Figure 8. Invasive growth phenotype of *ste20*Δ *urm1*Δ double mutants. Equal concentrations of strains SY3826 (WT), SY3828 (*urm1*Δ), SY3827 (*uba4*Δ), SY3834 (*ste20*Δ), SY3837 (*urm1*Δ *ste20*Δ), and SY3838 (*uba4*Δ *ste20*Δ) were spotted on YEPD plates and incubated at 30°C for 4 d. Plates were photographed, washed, and then photographed again.

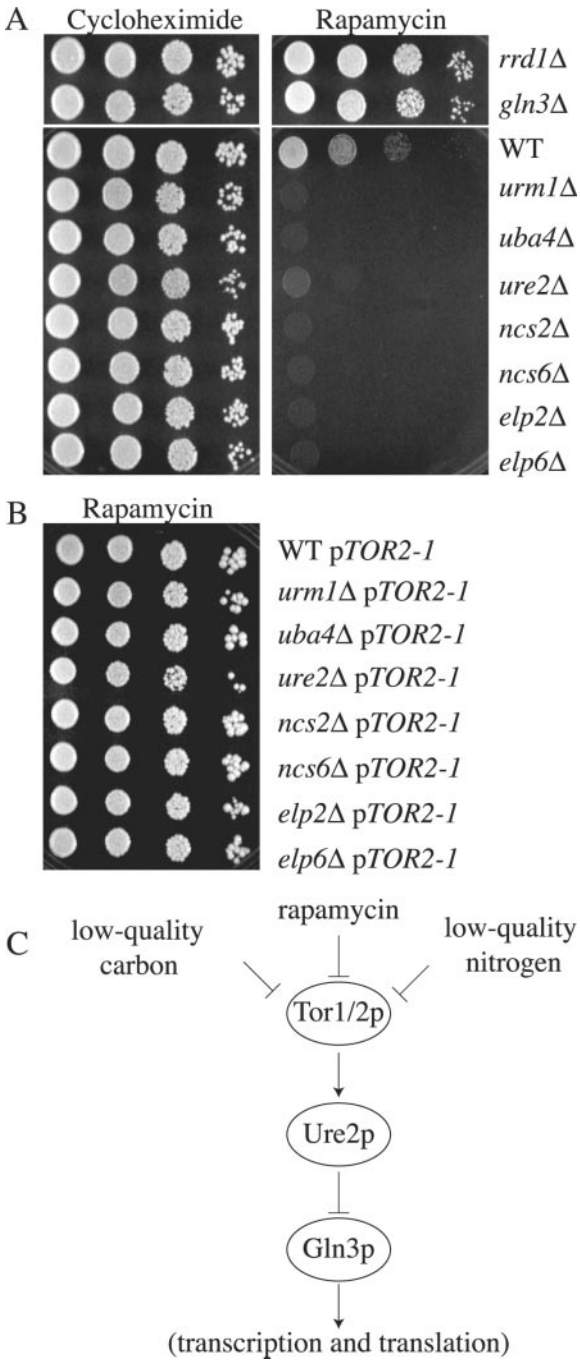

Figure 9. Interaction of the urmylation pathway with TOR signaling. Strains SY3835 (*ncs1*Δ), SY3836 (*gln3*Δ), BY4741 (wild type), SY3839 (*urm1*Δ), SY3840 (*uba4*Δ), SY3841 (*ncs2*Δ), SY3842 (*ncs6*Δ), SY3843 (*elp2*Δ), SY3844 (*elp6*Δ), and SY3845 (*ure2*Δ) were grown to mid-log in YEPD at 30°C. A serial dilution (1/10) was performed starting with 10,000 cells. Cells were spotted onto either YEPD + 100 nM cycloheximide (left) or YEPD + 25 nM rapamycin (right) and grown 3 d at 30°C. (B) Strains SY3835 (*ncs1*Δ), SY3836 (*gln3*Δ), BY4741 (wild type), SY3839 (*urm1*Δ), SY3840 (*uba4*Δ), SY3841 (*ncs2*Δ), SY3842 (*ncs6*Δ), SY3843 (*elp2*Δ), SY3844 (*elp6*Δ), and SY3845 (*ure2*Δ) carrying p*TOR2–1* (pML41) were grown to mid-log in YEPD at 30°C. A serial dilution (1/10) was performed starting with 10,000 cells. Cells were spotted YEPD + 25 nM rapamycin (right) and grown 3 d at 30°C. (C) A model for genetic interaction between TOR and other components in the rapamycin-sensitive pathway.

involved in invasive growth. Perhaps the loss of Ure2p results in misregulation of this gene, which in turn leads to a defect in invasion. In addition to the difference in the pattern of Urm1p conjugates, loss of Ure2p also has different physiological consequences from loss of Elp2, Elp6p, Ncs2p, and Ncs6p. The *ure2*Δ mutants are defective in both bud pattern (unipolar budding) and in cell elongation during invasive growth, whereas *elp2*Δ, *elp6*Δ, *ncs2*Δ, and *ncs6*Δ mutants were defective only in elongation. Finally, *ure2*Δ *cla4*Δ mutants arrest with a terminal phenotype in which the cells have elongated buds but properly localized septin rings. The *elp2*Δ cla4Δ, *elp6*Δ *cla4*Δ, *ncs2*Δ *cla4*Δ, and *ncs6*Δ *cla4*Δ mutants arrest as cells with elongated buds and mislocalized septins. Identification of the 131-kDa conjugate will help clarify why Ure2p is essential in a *cla4*Δ mutant, its role in invasion, and how Ure2p interacts with the urmylation pathway.

Connection between Urmylation, TOR Signaling, Invasive, and Pseudohypal Growth

We have shown that loss of *URM1*, *UBA4*, *URE2*, *ELP2*, *ELP6*, *NCS2*, and *NCS6* confers sensitivity to rapamycin. Perhaps these gene products serve as enhancers of TOR signaling or of a cellular process regulated by TOR. In addition, we found the urmylation pathway, as well as *URE2*, *ELP2*, *ELP6*, *NCS2*, and *NCS6*, plays a role in starvation response in haploids (invasive growth) and diploids (pseudohyphal growth). Given that glucose depletion results in invasive growth and pseudohyphal growth (Cullen and Sprague, 2000, 2002) and given that the TOR proteins directly modulate a glucose sensitive signaling pathway (Hardwick *et al*., 1999), perhaps the urmylation pathway links TOR signaling and these morphogenetic transitions.

Implications for Urmylation and TOR Signaling in Mammals

The TOR proteins are conserved from yeast to mammals and play a role in nutrient sensing. The mammalian target of rapamycin, mTOR, has been shown to link growth factor signaling and proteins involved in cell cycle progression (Brown *et al*., 1994; Chiu *et al*., 1994). In response to nitrogen availability, TOR regulates transcription and translation. Recent clinical advances suggest rapamycin may be a novel chemotherapy agent for rapamycin-sensitive tumors such as glioblastoma and prostate carcinoma (Shi *et al*., 1995; Hosoi *et al*., 1999; Louro *et al*., 1999). Moreover, addition of rapamycin has been shown to impair TOR-dependent cell proliferation in leukemic cells (Iiboshi *et al*., 1999). Intriguingly, based on homology, there seems to be a functional counterpart to Urm1p in mammals. Perhaps in mammals the urmylation pathway also functions in nutrient sensing. Clearly, much still remains to be learned about the connection between the urmylation pathway and the TOR regulation of nutrient signaling, but studies in yeast could provide insights into conserved pathways as targets for therapy.

ACKNOWLEDGMENTS

We thank for J. Pringle, J. Heitman, K. Arndt, and T. Stevens for providing plasmids and reagents. Thanks also to Paul Cullen, Hilary Kemp, Megan Keniry, Dave Mitchell, and Greg Smith for helpful comments and suggestions. This work was supported by a research grant (GM-30027 to G.F.S.) and training grants (HD-07348 to D.M.R. and GM-07759 to A.S.G) from the National Institutes of Health.

A

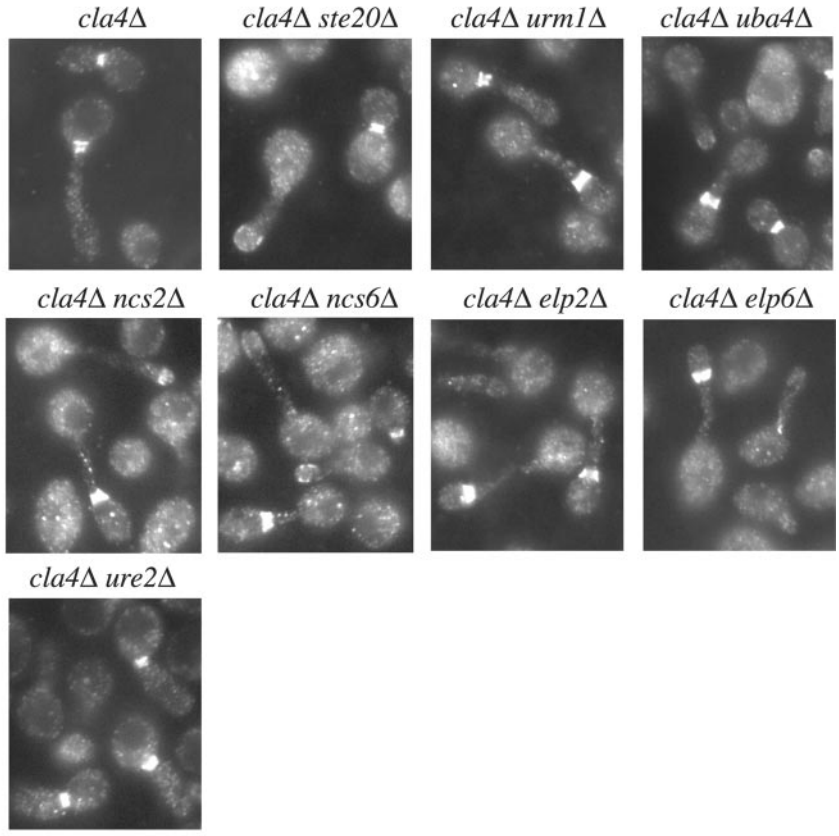

B

Cdc3p mislocalization

genotype	%mislocalization
cla4Δ (YCp*HIS3cla4-75*)	2
ste20Δ cla4Δ (YCp*HIS3cla4-75*)	46
urm1Δ cla4Δ (YCp*HIS3cla4-75*)	46
uba4Δ cla4Δ (YCp*HIS3cla4-75*)	45
ncs2Δ cla4Δ (YCp*HIS3cla4-75*)	46
ncs6Δ cla4Δ (YCp*HIS3cla4-75*)	40
elp2Δ cla4Δ (YCp*HIS3cla4-75*)	43
elp6Δ cla4Δ (YCp*HIS3cla4-75*)	48
ure2Δ cla4Δ (YCp*HIS3cla4-75*)	5

Figure 10. Terminal phenotype of cells lacking Ncs2p, Ncs6p, Elp6p, and Ure2p in a *cla4Δ* mutant strain. Exponential cultures of SY3380 (*cla4Δ*), SY3810 (*urm1Δ cla4Δ*), SY3809 (*uba4Δ cla4Δ*), SY3822 (*ncs2Δ cla4Δ*), SY3823 (*ncs6Δ cla4Δ*), SY3824 (*elp6Δ cla4Δ*), and SY3825 (*ure2Δ cla4Δ*) carrying YCp*HIS3cla4-75* were grown at 25°C in YEPD, shifted to 37°C for 4 h, fixed, and stained for Cdc3p. (B) Quantitation of Cdc3p mislocalization. For each strain, 250 cells were counted in three independent experiments.

REFERENCES

Adams, A.E., Johnson, D.I., Longnecker, R.M., Sloat, B.F., and Pringle, J.R. (1990). CDC42 and *CDC43*, two additional genes involved in budding and the establishment of cell polarity in the yeast *Saccharomyces cerevisiae*. J. Cell Biol. *111*, 131–142.

Barbet, N.C., Schneider, U., Helliwell, S.B., Stansfield, I., Tuite, M.F., and Hall, M.N. (1996). TOR controls translation initiation and early G1 progression in yeast. Mol. Biol. Cell *7*, 25–42.

Baudin, A., Ozier-Kalogeropoulos, O., Denouel, A., Lacroute, F., and Cullin, C. (1993). A simple and efficient method for direct gene deletion in *Saccharomyces cerevisiae*. Nucleic Acids Res. *21*, 3329–3330.

Beck, T., and Hall, M.N. (1999). The TOR signalling pathway controls nuclear localization of nutrient-regulated transcription factors. Nature *402*, 689–692.

Bertram, P.G., Choi, J.H., Carvalho, J., Ai, W., Zeng, C., Chan, T.F., and Zheng, X.F. (2000). Tripartite regulation of Gln3p by TOR, Ure2p, and phosphatases. J. Biol. Chem. *275*, 35727–35733.

Brown, E.J., Albers, M.W., Shin, T.B., Ichikawa, K., Keith, C.T., Lane, W.S., and Schreiber, S.L. (1994). A mammalian protein targeted by G1-arresting rapamycin-receptor complex. Nature *369*, 756–758.

Brown, J.L., Jaquenoud, M., Gulli, M.P., Chant, J., and Peter, M. (1997). Novel Cdc42-binding proteins Gic1 and Gic2 control cell polarity in yeast. Genes Dev. *11*, 2972–2982.

Cardenas, M.E., Cutler, N.S., Lorenz, M.C., Di Como, C.J., and Heitman, J. (1999). The TOR signaling cascade regulates gene expression in response to nutrients. Genes Dev. *13*, 3271–3279.

Chan, T.F., Carvalho, J., Riles, L., and Zheng, X.F. (2000). A chemical genomics approach toward understanding the global functions of the target of rapamycin protein (TOR). Proc. Natl. Acad. Sci. USA *97*, 13227–13232.

Chen, G.C., Kim, Y.J., and Chan, C.S. (1997). The Cdc42 GTPase-associated proteins Gic1 and Gic2 are required for polarized cell growth in *Saccharomyces cerevisiae*. Genes Dev. *11*, 2958–2971.

Chiu, M.I., Katz, H., and Berlin, V. (1994). RAPT1, a mammalian homolog of yeast Tor, interacts with the FKBP12/rapamycin complex. Proc. Natl. Acad. Sci. USA *91*, 12574–12578.

Cullen, P.J., and Sprague, G.F., Jr. (2000). Glucose depletion causes haploid invasive growth in yeast. Proc. Natl. Acad. Sci. USA *97*, 13619–13624.

Cullen, P.J., and Sprague, G.F., Jr. (2002). The roles of bud-site-selection proteins during haploid invasive growth in yeast. Mol. Biol. Cell *13*, 2990–3004.

Cvrckova, F., De Virgilio, C., Manser, E., Pringle, J.R., and Nasmyth, K. (1995). Ste20-like protein kinases are required for normal localization of cell growth and for cytokinesis in budding yeast. Genes Dev. *9*, 1817–1830.

Di Como, C.J., and Arndt, K.T. (1996). Nutrients, via the Tor proteins, stimulate the association of Tap42 with type 2A phosphatases. Genes Dev. *10*, 1904–1916.

Drubin, D.G., and Nelson, W.J. (1996). Origins of cell polarity. Cell *84*, 335–344.

Fellows, J., Erdjument-Bromage, H., Tempst, P., and Svejstrup, J.Q. (2000). The Elp2 subunit of elongator and elongating RNA polymerase II holoenzyme is a WD40 repeat protein. J. Biol. Chem. *275*, 12896–12899.

Furukawa, K., Mizushima, N., Noda, T., and Ohsumi, Y. (2000). A protein conjugation system in yeast with homology to biosynthetic enzyme reaction of prokaryotes. J. Biol. Chem. *275*, 7462–7465.

Gietz, R.D., Schiestl, R.H., Willems, A.R., and Woods, R.A. (1995). Studies on the transformation of intact yeast cells by the LiAc/SS-DNA/PEG procedure. Yeast *11*, 355–360.

Gimeno, C.J., Ljungdahl, P.O., Styles, C.A., and Fink, G.R. (1992). Unipolar cell divisions in the yeast *S. cerevisiae* lead to filamentous growth: regulation by starvation and. RAS. Cell *68*, 1077–1090.

Goehring, A.S., Mitchell, D.A., Tong, A.H., Keniry, M.E., Boone, C., and Sprague, G.F., Jr. (2003). Synthetic lethal analysis implicates Ste20p, a p21-activated protein kinase, in polarisome activation. Mol. Biol. Cell *14*, 1501–1516.

Haas, A.L., and Bright, P.M. (1988). The resolution and characterization of putative ubiquitin carrier protein isozymes from rabbit reticulocytes. J. Biol. Chem. *263*, 13258–13267.

Haas, A.L., Bright, P.M., and Jackson, V.E. (1988). Functional diversity among putative E2 isozymes in the mechanism of ubiquitin-histone ligation. J. Biol. Chem. *263*, 13268–13275.

Hardwick, J.S., Kuruvilla, F.G., Tong, J.K., Shamji, A.F., and Schreiber, S.L. (1999). Rapamycin-modulated transcription defines the subset of nutrient-sensitive signaling pathways directly controlled by the Tor proteins. Proc. Natl. Acad. Sci. USA *96*, 14866–14870.

Harlow, E., and Lane, D. (1988). Antibodies: A Laboratory Manual, Cold Spring Harbor, NY: Cold Spring Harbor Laboratory Press.

Helliwell, S.B., Wagner, P., Kunz, J., Deuter-Reinhard, M., Henriquez, R., and Hall, M.N. (1994). TOR1 and TOR2 are structurally and functionally similar but not identical phosphatidylinositol kinase homologues in yeast. Mol. Biol. Cell *5*, 105–118.

Hochstrasser, M. (2000). Evolution and function of ubiquitin-like protein-conjugation systems. Nat. Cell Biol. *2*, E153–157.

Hosoi, H., Dilling, M.B., Shikata, T., Liu, L.N., Shu, L., Ashmun, R.A., Germain, G.S., Abraham, R.T., and Houghton, P.J. (1999). Rapamycin causes poorly reversible inhibition of mTOR and induces p53-independent apoptosis in human rhabdomyosarcoma cells. Cancer Res. *59*, 886–894.

Ichimura, Y., *et al*. (2000). A ubiquitin-like system mediates protein lipidation. Nature *408*, 488–492.

Iiboshi, Y., Papst, P.J., Hunger, S.P., and Terada, N. (1999). L-Asparaginase inhibits the rapamycin-targeted signaling pathway. Biochem. Biophys. Res. Commun. *260*, 534–539.

Johnson, D.I., and Pringle, J.R. (1990). Molecular characterization of *CDC42*, a *Saccharomyces cerevisiae* gene involved in the development of cell polarity. J. Cell Biol. *111*, 143–152.

Johnson, E.S., Schwienhorst, I., Dohmen, R.J., and Blobel, G. (1997). The ubiquitin-like protein Smt3p is activated for conjugation to other proteins by an Aos1p/Uba2p heterodimer. EMBO J. *16*, 5509–5519.

Kawakami, T., *et al*. (2001). NEDD8 recruits E2-ubiquitin to SCF E3 ligase. EMBO J. *20*, 4003–4012.

Kim, H.B., Haarer, B.K., Pringle, J.R. (1991). Cellular morphogenesis in the Saccharomyces cerevisiae cell cycle: localization of the CDC3 gene product and the timing of events at the budding site. J. Cell. Biol. *112*, 535–544.

Komeili, A., Wedaman, K.P., O'Shea, E.K., and Powers, T. (2000). Mechanism of metabolic control. Target of rapamycin signaling links nitrogen quality to the activity of the Rtg1 and Rtg3 transcription factors. J. Cell Biol. *151*, 863–878.

Krogan, N.J., and Greenblatt, J.F. (2001). Characterization of a six-subunit holo-elongator complex required for the regulated expression of a group of genes in *Saccharomyces cerevisiae*. Mol. Cell Biol. *21*, 8203–8212.

Kunz, J., Henriquez, R., Schneider, U., Deuter-Reinhard, M., Movva, N.R., and Hall, M.N. (1993). Target of rapamycin in yeast, TOR2, is an essential phosphatidylinositol kinase homolog required for G1 progression. Cell *73*, 585–596.

Kuruvilla, F.G., Shamji, A.F., Sternson, S.M., Hergenrother, P.J., and Schreiber, S.L. (2002). Dissecting glucose signalling with diversity-oriented synthesis and small-molecule microarrays. Nature *416*, 653–657.

Lammer, D., Mathias, N., Laplaza, J.M., Jiang, W., Liu, Y., Callis, J., Goebl, M., and Estelle, M. (1998). Modification of yeast Cdc53p by the ubiquitin-related protein Rub1p affects function of the SCFCdc4 complex. Genes Dev. *12*, 914–926.

Leberer, E., Wu, C., Leeuw, T., Fourest-Lieuvin, A., Segall, J.E., and Thomas, D.Y. (1997). Functional characterization of the Cdc42p binding domain of yeast Ste20p protein kinase. EMBO J. *16*, 83–97.

Li, R., Zheng, Y., and Drubin, D.G. (1995). Regulation of cortical actin cytoskeleton assembly during polarized cell growth in budding yeast. J. Cell Biol. *128*, 599–615.

Li, S.J., and Hochstrasser, M. (2000). The yeast *ULP2* (*SMT4*) gene encodes a novel protease specific for the ubiquitin-like Smt3 protein. Mol. Cell Biol. *20*, 2367–2377.

Liakopoulos, D., Doenges, G., Matuschewski, K., and Jentsch, S. (1998). A novel protein modification pathway related to the ubiquitin system. EMBO J. *17*, 2208–2214.

Longtine, M.S., McKenzie, A., Demarini, D.J., Shah, N.G., Wach, A., Brachat, A., Philippsen, P., and Pringle, J.R. (1998). Additional modules for versatile and economical PCR-based gene deletion and modification in *Saccharomyces cerevisiae*. Yeast *14*, 953–961.

Lorenz, M.C., and Heitman, J. (1995). TOR mutations confer rapamycin resistance by preventing interaction with FKBP12-rapamycin. J. Biol. Chem. *270*, 27531–27537.

Louro, I.D., McKie-Bell, P., Gosnell, H., Brindley, B.C., Bucy, R.P., and Ruppert, J.M. (1999). The zinc finger protein GLI induces cellular sensitivity to the mTOR inhibitor rapamycin. Cell Growth Differ. *10*, 503–516.

Ma, H., Kunes, S., Schatz, P.J., and Botstein, D. (1987). Plasmid construction by homologous recombination in yeast. Gene *58*, 201–216.

Mahajan, R., Delphin, C., Guan, T., Gerace, L., and Melchior, F. (1997). A small ubiquitin-related polypeptide involved in targeting RanGAP1 to nuclear pore complex protein RanBP2. Cell *88*, 97–107.

Mahajan, R., Gerace, L., and Melchior, F. (1998). Molecular characterization of the SUMO-1 modification of RanGAP1 and its role in nuclear envelope association. J. Cell Biol. *140*, 259–270.

Mitchell, D.A., and Sprague, G.F. (2001). The phosphotyrosyl phosphatase activator, Ncs1p (Rrd1p), functions with Cla4p to regulate the G(2)/M transition in *Saccharomyces cerevisiae*. Mol. Cell Biol. *21*, 488–500.

Peter, M., Neiman, A.M., Park, H.O., van Lohuizen, M., and Herskowitz, I. (1996). Functional analysis of the interaction between the small GTP binding protein Cdc42 and the Ste20 protein kinase in yeast. EMBO J. *15*, 7046–7059.

Rempola, B., Kaniak, A., Migdalski, A., Rytka, J., Slonimski, P.P., and di Rago, J.P. (2000). Functional analysis of *RRD1* (YIL153w) and *RRD2* (YPL152w), which encode two putative activators of the phosphotyrosyl phosphatase activity of PP2A in *Saccharomyces cerevisiae*. Mol. Gen. Genet. *262*, 1081–1092.

Richman, T.J., and Johnson, D.I. (2000). Saccharomyces cerevisiae Cdc42p GTPase is involved in preventing the recurrence of bud emergence during the cell cycle. Mol. Cell Biol. *20*, 8548–8559.

Roberts, R.L., and Fink, G.R. (1994). Elements of a single MAP kinase cascade in *Saccharomyces cerevisiae* mediate two developmental programs in the same cell type: mating and invasive growth. Genes Dev. *8*, 2974–2985.

Rose, M.D., Winston, F., and Hieter, P. (ed) (1990). Methods in Yeast Genetics, Cold Spring Harbor, NY: Cold Spring Harbor Laboratory Press.

Sambrook, J., Fritsch, E.F., and Maniatis, T. (1989). Molecular Cloning: A Laboratory Manual, Cold Spring Harbor, NY: Cold Spring Harbor Laboratory Press.

Shi, Y., Frankel, A., Radvanyi, L.G., Penn, L.Z., Miller, R.G., and Mills, G.B. (1995). Rapamycin enhances apoptosis and increases sensitivity to cisplatin *in vitro.* Cancer Res. *55*, 1982–1988.

Sikorski, R.S., and Hieter, P. (1989). A system of shuttle vectors and yeast host strains designed for efficient manipulation of DNA in *Saccharomyces cerevisiae.* Genetics *122*, 19–27.

Winkler, G.S., Kristjuhan, A., Erdjument-Bromage, H., Tempst, P., and Svejstrup, J.Q. (2002). Elongator is a histone H3 and H4 acetyltransferase important for normal histone acetylation levels *in vivo.* Proc. Natl. Acad. Sci. USA *99*, 3517–3522.

Winkler, G.S., Petrakis, T.G., Ethelberg, S., Tokunaga, M., Erdjument-Bromage, H., Tempst, P., and Svejstrup, J.Q. (2001). RNA polymerase II elongator holoenzyme is composed of two discrete subcomplexes. J. Biol. Chem. *276*, 32743–32749.

Ziman, M., Preuss, D., Mulholland, J., O'Brien, J.M., Botstein, D., and Johnson, D.I. (1993). Subcellular localization of Cdc42p, a *Saccharomyces cerevisiae* GTP-binding protein involved in the control of cell polarity. Mol. Biol. Cell *4*, 1307–1316.